Differential origin of the activation of dorsal and ventral dentate gyrus granule cells during paradoxical (REM) sleep in the rat

Francesca Billwiller, Leslie Renouard, Patrice Fort, Pierre-Hervé Luppi

Differential origin of the activation of dorsal and ventral dentate gyrus granule cells during paradoxical (REM) sleep in the rat

Francesca Billwiller [1], Leslie Renouard [1], Olivier Clement[1], Patrice Fort[1] and Pierre-Hervé Luppi[1]*

[1]*UMR 5292 CNRS/U1028 INSERM, Centre de Recherche en Neurosciences de Lyon (CRNL), SLEEP Team, Université Claude Bernard Lyon I, Faculté de Médecine RTH Laennec, 7 Rue Guillaume Paradin, 69372 LYON Cedex 08, France.*

Number of text pages: 19

Number of Figures: 5

Number of Tables: 1

* Corresponding author : Dr Pierre-Hervé Luppi

Team SLEEP, UMR *5292 CNRS/U1028 INSERM*,

7, Rue Guillaume Paradin, 69372 LYON cedex 08, FRANCE

Tel number: (+33) 4 78 77 10 40

Fax number: (+33) 4 78 77 10 22

E-mail address: luppi@sommeil.univ-lyon1.fr

Acknowledgments: This work was supported by CNRS, Fondation pour la recherche médicale (FRM), Societé Francaise de Recherche et Médecine du Sommeil (SFRMS) and University Claude Bernard of Lyon

Abstract:

We recently demonstrated that granule cells located in the dorsal dentate gyrus (dDG) are activated by neurons located in the lateral supramammillary nucleus (SumL) during paradoxical sleep (PS) hypersomnia. To determine whether these neurons are glutamatergic

and/or GABAergic, we combined FOS immunostaining with *in situ* hybridization of vesicular glutamate transporter 2 (vGLUT2, a marker of glutamatergic neurons) or that of the vesicular GABA transporter (vGAT, a marker of GABAergic neurons) mRNA in rats displaying PS hypersomnia (PSR). We found that 84% and 76% of the FOS+ SumL neurons in PSR rats expressed vGLUT2 and vGAT mRNA, respectively. Then, we examined vGLUT2 and FOS immunostaining in the dorsal and ventral DG of PSR rats with a neurochemical lesion of the Sum. In PSR lesioned animals but not in sham animals, nearly all vGLUT2+ fibers and FOS+ neurons disappeared in the dDG but not in the ventral DG (vDG). To identify the pathway (s) responsible (s) for the activation of the vDG during PS hypersomnia, we combined Fluorogold (FG) injection in the vDG of PSR rats with FOS staining. We found a large number of neurons FOS-FG+ specifically in the medial entorhinal cortex (ENTm). Altogether, our results suggest that SumL neurons with a unique dual glutamatergic and GABAergic phenotype are responsible for the activation of the dDG during PS hypersomnia while vDG granule neurons are activated by ENTm cortical neurons. These results suggest differential mechanisms and functions for the activation of the dDG and the vDG granule cells during PS.

Introduction

Paradoxical (REM) sleep (PS) is characterized by muscle atonia, rapid eye movements (REM) and cortical and hippocampal activation (Jouvet et al. 1959). We recently showed that the dentate gyrus (DG) is strongly activated during PS. Indeed, a large number of neurons with an increased expression of FOS, BDNF, COX2 and ARC, known markers of activation and/or synaptic plasticity are selectively observed specifically in the DG in PS hypersomniac rats compared to control and PS deprived animals (Renouard et al. 2015). We further found out combining FOS labelling after PS hypersomnia with retrograde tracer injection in the dorsal part of the DG (dDG) that the lateral part of the supramammillary nucleus (SumL) is the only brain structure containing a large number of double-labelled neurons. Finally, we showed that a neurotoxic lesion of the Sum drastically decreases the number of FOS+ granule cells in the dDG in PS hypersomniac animals (Renouard et al. 2015). These results suggest that SumL neurons are responsible for the activation of dDG granule cells during PS hypersomnia. Still,

the neurotransmitter content of these neurons remained to be identified. A number of results suggested that they might display a unique dual glutamatergic and GABAergic phenotype. Indeed, after injection of the anterograde tracer BDA in the SumL, all terminals located in the dDG coexpressed vesicular GABA/glycine transporter (vGAT) and vesicular 2 glutamate transporter (vGLUT2), markers of GABAergic and glutamatergic neurons, respectively. The ventral dentate gyrus (vDG) contained less GABA/glutamate terminals coming from the SumL and received additional strictly glutamatergic projection from the medial part of the Sum (SumM)(Soussi et al. 2010). In view of all these results, our aim in the present study was to determine whether the SumL neurons expressing FOS during PS hypersomnia are indeed glutamatergic and GABAergic and whether they can be also responsible for the activation of the ventral DG (vDG) in addition to that of the dDG. To this aim, we used a combination of FOS immunostaining and *in situ* hybridization of vGLUT2 or vGAT mRNA in PS hypersomniac rats (PSR). In addition, we analyzed the distribution of the vGLUT2+ fibers and of the FOS+ neurons in the dDG and vDG of PSR animals after neurotoxic lesions of the Sum. Finally, we combined FOS labelling in PSR rats with retrograde tracer injection in the vDG.

Materials and Methods

All experiments were conducted in accordance to the French and European Community guidelines for the use of animals in research and approved by the institutional animal care and use committee of the University of Lyon 1 (protocols BH 2006-09 and BH 2006-10).
Sprague-Dawley male rats were housed individually in recording barrels under a constant 12h light-dark cycle (light on from 07:00 AM to 07:00 PM). Room temperature was maintained at 21±1°C, and standard rodent food and water were available *ad libitum* throughout the experiment.

Animals and surgery

28 Male Sprague-Dawley rats (260-300 g, Charles River, n=12 for vGLUT2/FOS staining, n=4 for vGAT/FOS staining, n=8 for lesions experiments, n= 4 for Fluorogold injections) were implanted with electroencephalographic (EEG) and electromyographic (EMG) electrodes under ketamine (Virbac Santé Animale, 100 mg/kg, i.p) and xylazine (Bayer, 50 mg/kg, i.p) anaesthesia. Lidocaïne (Xylovet, Ceva Santé Animale) injected subcutaneously was used for analgesia. Three stainless steel screws were fixed in the parietal, frontal and occipital parts of the skull while the reference electrode for unipolar EEG recording was fixed on the cerebellum bone. Two wire electrodes were inserted into the neck muscles for bipolar EMG recordings. All leads were connected to a miniature plug (Plastics One Inc.) that was cemented on the skull.

Lesion

Male Sprague-Dawley rats (260-300 g, Charles River) were anesthetized as described above and placed in a stereotaxic apparatus. The lesions were made bilaterally in four rats by passing a 10 µA continuous current for 10 min through a micropipette containing ibotenic acid (25 mmol/L in distilled water adjusted at pH 8, Tocris) in each Sum (coordinates: AP: -4.5 mm to Bregma, ML: +0.6 mm lateral to midline, DP: 8.3 mm from the brain surface). Four sham rats were subjected to the same protocol with a micropipette containing 0.9% NaCl. All animals were then implanted for EEG and EMG recordings as described above.

Tracer injections

Male Sprague-Dawley rats (260-300 g, Charles River, n=4) were anesthetized as described above and placed in a stereotaxic apparatus. Glass micropipettes (4-5 µm O.D.) were backfilled with Fluorogold (FG, Fluoprobe, diluted in distilled water at 8 mmol/L and pH 6) and lowered in the vDG (coordinates: AP -6 mm to Bregma, ML +4.1 mm lateral to midline, DP: 6.8 mm from the brain surface). FG was ejected during 15 min with a continuous current of +2 µA. Animals were then implanted for EEG and EMG recordings as described above and submitted to PS deprivation and recovery procedure (see below) before being perfused.

Polygraphic recordings

Animals recovered from surgery during one week in a plexiglas jar before being habituated to the recording conditions for three days. Rats were connected to a cable attached to a slip-ring commutator to allow free movement of the animal within the jar. EEG and EMG recordings were collected on a computer via a CED interface using the Spike 2 software (Cambridge Electronic Design, Cambridge, UK).

PS deprivation and recovery protocol

PS deprivation was performed using the flowerpot method (Verret et al. 2003). Rats were divided in 3 groups: control (PSC, n=4), deprived of PS for 3 days (PSD, n=4) and rats allowed recovering after such deprivation (PSR, n=20). PSC animals remained in their standard cage throughout the experiment. After 48 h of baseline recordings, PSD and PSR rats were placed at 10:00 AM in a standard container filled with water (2-3 cm depth) and containing three platforms (6.2 cm diameter, 7-12 cm height) spaced 7-8 cm apart, so that rats were able to easily move between them. For the FOS-vGLUT2, FOS-vGAT and FOS-FG experiments, animals were put on a single platform. During PSD, food and water were available *ad libitum* and the container was cleaned daily. The third day, PSR animals were removed from their cages at 10:00 AM and put on a dry bed of woodchips in recording jars to allow PS recovery. The animals used for the FOS-vGLUT2, FOS-vGAT and FOS-FG experiment were perfused three hours and the other PSR animals six hours after the onset of PS recovery.

Perfusion, fixation and sectioning

Animals were perfused with a Ringer's lactate solution containing 0.1% heparin followed by 500 ml of a fixative solution composed of 4% paraformaldehyde in 0.1 M phosphate buffer (PB, pH 7.4). Brains were postfixed for 12 h at 4°C and then stored for 2 days at 4°C in a PB buffer containing 30% sucrose and 0.1% sodium azide (Sigma-Aldrich). Brains were rapidly frozen in methylbutane (Sigma-Aldrich) cooled with dry ice and sliced on a cryostat (Microm). For immunohistochemistry experiments, brains were cut in 25 µm-thick coronal sections and stored in PB containing 0.9% NaCl, 0.3% Triton X-100 and 0.1% sodium azide (PBST-Az). For *in situ* hybridization experiments, brains were cut in 30 µm-thick coronal sections and stored at -20°C in an RNAse-free cryoprotectant solution consisting of 20%

Glycerol, 30% Ethylene Glycol and 0.05% RNase inhibitor in a 50 mM potassium-phosphate buffer (Sigma-Aldrich).

FOS immunohistochemistry combined with vGLUT2 or vGAT *in situ* hybridization

The recombinant plasmid (pCRII-TOPO, Invitrogen) containing the vGLUT2 cDNA was linearized using Not I and Hind III (New England Biolabs) and transcribed using SP6 and T7 RNA polymerases (for antisens and sens riboprobes, respectively). The vGAT riboprobes were prepared by PCR as previously described (Gandrillon et al. 1996). All riboprobes were transcribed using a non-radioactive RNA labelling kit (Roche Diagnostic) following manufacturer's instructions. Digoxigenin-labelled riboprobes were then stored at -20°C in a hybridization buffer. As described before (Sapin et al. 2009), brain sections were successively incubated with a rabbit antiserum to FOS (1:3000 for vGLUT2, 1:4000 for vGAT, Merck), in 10 mM PB containing 0.9% NaCl and 0.3% Triton-100x (PBST) for 18 h at room temperature; a biotinylated goat anti-rabbit IgG solution (1:1000, Vector Laboratories) and an ABC-HRP solution (1:1000, Elite kit, Vector Laboratories), both for 90 min at room temperature. Then, sections were immersed for around 15 min in a 0.05 M Tris-HCl buffer containing 0.025% 3,3-diaminobenzidine-4 HCl (DAB, Sigma-Aldrich) and 0.003% H_2O_2. Sections were rinsed 3 times in PBST between each step. Then, they were incubated in PBST containing 10 mM dithio-threitol (DTT, Sigma-Aldrich) twice for 10 min and in a standard saline citrate solution (SSC 2X) for 10 min. All the buffers excepting DTT contained 0.2% of RNase inhibitor (Sigma-Aldrich). Sections were then placed overnight at 65°C in the hybridization buffer consisting of 150 mM NaCl, 8 mM Tris-HCl, 1 mM Tris-Base, 6 mM NaH_2PO_4, 5 mM Na_2HPO, 5 mM EDTA, 50% formamide, 10% dextran sulphate, yeast tRNA (Sygma type III, 1 mg/ml, Sigma-Aldrich), 0.02% ficoll, 0.02% polyvinylpyrorolidone containing 0.5 µg/mL of the digoxigenin-labeled probe. Sections were washed in SSC 1X, 50% formamide, 0.1% Tween-20 twice for 20 min at 55°C and treated with 10 µg/µl RNase A (USB Corporation) in Tris 10 mM containing 1 mM EDTA and 500 mM NaCl for 15 min at 37°C. After 3 washes in PBST, sections were incubated overnight with an anti-digoxigenin antibody conjugated to alkaline phosphatase (1:2000, Roche Diagnostic) in PBST containing 0.2% blocking agent (Roche Diagnostic). Then, they were washed twice in PBST, once in PBS 10 mM, and in a buffer containing 1 M Tris-HCl, 1 M NaCl, 500 mM $MgCl_2$, and 1% Tween-20. Each washing lasted 10 min. Sections were then incubated at 37°C in the same buffer containing nitroblue tetrazolium (NBT) and 5-bromo-4-chloro-3-indolyl-phosphate

(BCIP) (20 µl/ml, Roche Diagnostic). After ~4 h of incubation in the revelation buffer, sections were washed in PBST twice for 10 min. Finally, the sections were mounted on glass slides, dried and coverslipped with Vectamount (Vector Laboratories). Controls in the absence of primary antibodies (anti-FOS and anti-digoxigenin) or with the sense probe were run to ensure the specificity of the labelling.

vGLUT2, FOS, FOS-FG and NeuN immunohistochemistry

Sections of PSR rats were incubated in a rabbit antiserum to vGLUT2 (1:10000, Synaptic Systems) or to FOS (1:5000 for PSR lesion and sham rats, 1:10000 for PSR rats injected with FG, Merck) in PBST-Az for 3 days at 4°C. Then, sections were incubated in a biotinylated antirabbit IgG solution (1:1000 in PBST, Vector Labs) and an ABC-HRP solution (1:1000 in PBST; Elite kit, Vector Labs) for 90 min at room temperature. Finally, sections were immersed in a 0.05 M Tris-HCl buffer (pH 7.6) containing 0.025% 3,3'-diaminobenzidine-4 HCl (DAB, Sigma), 0.003% H_2O_2 and 0.6% nickel ammonium sulphate to obtain a black reaction product. Sections were rinsed 3 times in PBST between each step. FOS stained sections of PSR rats injected with FG were incubated in the rabbit antiserum to FG (1:15000, US Biological) in PBST-Az for 3 days at 4°C. Then, sections were incubated in a biotinylated antirabbit IgG solution (1:1000 in PBST, Vector Labs) and an ABC-HRP solution (1:1000 in PBST, Elite kit, Vector Labs) for 90 min at room temperature before being immersed in a DAB solution without nickel to obtain a brown reaction product.
Sections at the level of the Sum in lesion and sham animals were incubated in a mouse antiserum to NeuN (1:20000, Chemicon), followed by an incubation in a biotinylated antimouse IgG solution (1:1000 in PBST, Vector Labs), ABC-HRP solution and DAB nickel. Sections were then mounted and counterstained with neutral red.

Analysis of the sleep wake states

Vigilance states were discriminated using EEG and EMG data as previously described (Sapin et al. 2009). State classification was done by a visual check of polygraphic signals. For each rat, the last 3 or 6 hours of EEG/EMG recordings before perfusion were analyzed by 5 sec epochs in order to determine quantities of waking (WK), slow wave sleep (SWS) and PS. WK was characterized by a low-amplitude EEG and a sustained EMG activity; SWS was identified by high-voltage slow waves (1.5– 4.0 Hz) and spindles (10–14 Hz) without phasic

muscle activity; PS was characterized by theta rhythm (4–9 Hz) and muscle atonia. Hypnograms were obtained by using Spike-2 software (CED).

Analysis of immunostaining

The atlas of Swanson was used as a reference for all structures (Swanson 1992).
Drawings of double- or single-labelled sections were made with an Axioscope microscope (Zeiss) equipped with a motorized X–Y-sensitive stage and a video camera connected to a computerized image analysis system (Mercator, ExploraNova). The number of double labelled FOS-vGLUT2+, FOS-vGAT+ and FOS-FG+ neurons was quantified on 2 hemi-sections at the level of the Sum for all animals (-4.45 and -4.60 mm to Bregma). The number of double-labelled FOS-FG+ neurons was also quantified on 2 hemi-sections at the level of the medial septum (MS) and the diagonal band nucleus (NBD, +0.10 and -0.26 mm to Bregma), the lateral hypothalamic area (LHA, -3.25 and -3.90 mm to Bregma), the entorhinal cortex (ENT, -6.50 and -7.10 mm to Bregma) and the interpeduncular nucleus (IPN, -6.06 and -6.85 mm to Bregma).
In the DG, the number of FOS+ neurons and the level of expression of the vGLUT2 protein evaluated by optical density were quantified on 4 hemi-sections: -3.90 and -5 mm to Bregma for the dDG; -5.65 and -6.06 mm to Bregma for the vDG. Optical density was determined using ImageJ software in the granular layer of the DG and normalized using the DG molecular layer reading.

Statistical analysis

Analysis of variance (Kruskal-Wallis test following by Mann-Whitney tests) was performed on the different vigilance states, the number of labelled neurons and on the staining of vGLUT2 fibers for each structure across the experimental conditions (PSC, PSD, PSR, PSR-Sham and PSR-Lesion). All statistics were performed using Statview software.

Results

Quantification of Sleep

During the last 150 min before sacrifice, PSR animals used for FOS-vGLUT2 (n=4), FOS-vGAT (n=4) and FOS-FG experiments (n=4) spent significantly more time in PS than PSC (n=4) (39.1±2.4% and 7.05±1.8%, respectively, P=0.0041) and PSD (n=4) (1.5±1.5%, P=0.0041) animals (Fig. 1c). PSD rats spent significantly less time in PS than PSC rats (P=0.0433, Fig. 1e, f). PSR animals exhibited significantly less WK (18.3±3.4%) than PSC (49.3±8.5%, P=0.0188) and PSD (66.8±4.6%, P=0.0041) animals (Fig. 1a, b). No difference in SWS quantities was observed between the 3 groups of animals (PSC: 43.6±7.0%, PSD: 31.7±3.1%, PSR: 42.5±2.7%, P=0.0873, Fig. 1c, d). The PSR-lesioned (n=4) and sham rats (n=4) displayed the same amounts of PS, SWS and WK either in baseline condition (P=0.1489, =0.3865, =0.3865, respectively) or during PS hypersomnia (P= 0.0833, >0.9999, =0.1489, respectively).

Distribution of the FOS+, FOS/vGLUT2+ and FOS/vGAT+ double-labelled neurons in the supramammillary nucleus

To determine the level of activity of Sum neurons during PS hypersomnia, we quantified the number of neurons immunopositive for FOS in PSC (n=4), PSD (n=4) and PSR rats (n=4).
As previously shown (Renouard et al. 2015; Sapin et al. 2010), a large number of FOS-labelled cells was counted in the SumL specifically in PSR rats (P=0.0308, Table 1).
In contrast, a small and similar number of FOS labelled cells was observed between the three groups of animals in the SumM (P=0.1462, Table 1).
To identify the neurochemical nature of the Sum neurons activated during PS hypersomnia, we compared the distribution of FOS/vGLUT2+ neurons in PSC, PSD and PSR rats. No difference in the number of FOS/vGLUT2 double-labelled cells was observed in the SumM between the 3 groups of animals (PSC: 5.2±3.3, PSD: 15.2±5, PSR: 12±4.4, P=0.2468 (Table 1, Fig. 2a-c, e-f). In contrast, the number of FOS/vGLUT2 double-labelled cells was significantly higher in the SumL of PSR (94.5±11.9) than of PSC (22±8, P=0.0209) and PSD animals (29.5±11.5, P=0.0209). The double-labelled cells in the SumL constituted 84.2% of the total number of FOS+ cells in PSR animals (Table 1, Fig. 2a-c, e-f). Since it has been shown that vGAT colocalizes with vGLUT2 in SumL neurons, we additionally counted the number of FOS/vGAT+ neurons in the Sum of another group of PSR rats (n=4). We found that 76% of the FOS+ cells located in the SumL were vGAT+ in PSR animals (109±25.1, Fig. 2d, g-h). In contrast, a few FOS-vGAT double-labelled neurons was observed in the SumM of PSR rats (5.5±0.9).

Effect of Sum lesion on the distribution of the vGLUT2 labelled fibers in the dentate gyrus

We compared the level of expression of the vGLUT2 protein in the dDG and vDG of PSR rats with a bilateral iontophoretic injection of ibotenic acid (n=4) or NaCl (n=4) in the Sum. The Sum was left intact in PSR sham animals while it was entirely lesioned in those injected with ibotenic acid (Fig. 3i). In sham animals, a very high number of vGLUT2 immunoreactive fibers were localized in the supragranular layer of the DG whereas nearly no fibers were observed in the molecular and the polymorph layers (Fig. 3a, 4a).

In the PSR lesioned rats, very few vGLUT2+ fibers remained in the dDG and a strong reduction of the optic density (relative staining: 28.1±3.6) was measured compared to PSR sham rats (relative staining: 100±14.6, P=0.0209, Fig. 3a-d, j). In contrast, only a small non significant decrease in the optic density was found in the vDG between the two groups of animals (PSR lesioned: 87.6±7.4, PSR sham: 100±25.5, P=0.3865, Fig. 4a-d, j). However, the distribution of vGLUT2 fibers was not similar in the vDG of lesioned and sham rats. Indeed, vGLUT2 staining strongly decreased specifically in the supragranular layer of the DG and remained similar in the granular layer itself (Fig. 4a-d).

Number of FOS+ neurons in the dorsal and ventral dentate gyrus of PSR rats with a Sum lesion

The number of FOS+ neurons was strongly and significantly decreased in the dDG of the lesioned compared to the sham rats (20.2±6.4 versus 153.7±18.8, P=0.0209, Fig 3e-h, j, Fig. 4i). In contrast, only a small non significant decrease in the number of FOS+ neurons was observed in the vDG in the lesioned (235.2±27.2) versus the sham rats (311±23, P=0.0833, Fig. 4e-j).

Localization of the FOS+ neurons projecting to the vDG in PSR animals

After FG injection in the vDG (n=4, Fig 5g), only a small number of double-labelled cells were observed in the SumL (4±1.1). No or only a few number of double-labelled neurons were observed in other afferent structures to the vDG, like the medial septum (MS, 2.2±0.6),

the lateral hypothalamus (LHA, 4.5±1.7), the SumM (0.5±0.3), the lateral entorhinal cortex (ENTl, 3.2±1.9) and the interpeduncular nucleus (IPN, 1.7±0.6)(Fig 5h). In contrast, a very large number of double-labelled FG/FOS+ cells was observed in the medial entorhinal cortex (ENTm, 128.2±32.4). The double-labelled cells constituted 37.2±7.4% and 19±2.5 % of the total number of FG and FOS+ cells, respectively.

Discussion

We report here for the first time that around 80% of the FOS+ neurons localized in the SumL after PS hypersomnia express vGLUT2 or vGAT mRNA strongly suggesting that they are coexpressed in the same cells. We further demonstrate that all vGLUT2 fibers localized in the dorsal but not the ventral DG originate from the Sum. Besides, we show that the Sum is responsible for the activation of the dorsal but not the ventral DG granule cells during PS hypersomnia. Finally, we demonstrate that the ENTm contains a very large number of FOS+ neurons projecting to the vDG in PSR rats. Altogether, our results indicate that during PS hypersomnia GABA/glutamatergic neurons located in the SumL activate dDG granule cells while neurons located in ENTm activate vDG granule cells.

Our results complete and extend our previous studies showing in rats the presence of numerous FOS-labelled cells in the dorsal part of the DG and in the SumL after PS hypersomnia (Renouard et al. 2015; Sapin et al. 2010). We further show for the first time that 84 and 76% of the SumL FOS-labelled neurons express vGLUT2 and vGAT, respectively. Although a technologically challenging triple staining would be necessary to directly prove it, our results strongly suggest that SumL neurons activated during PS have a dual GABA/glutamatergic phenotype. In agreement with our results, it has been shown that a large number of SumL neurons express GAD65 (Soussi et al. 2010). In addition, using retrograde tracing of [3H]D-aspartate from the DG, numerous labelled neurons have been observed in the SumL suggesting that the SumL-DG pathway is glutamatergic (Kiss et al. 2000). Further, 86% of the total number of retrogradely labelled neurons located in the SumL after an injection of a retrograde tracer in the dDG expresses GAD65 mRNA (Soussi et al. 2010). We also previously showed that 28% of the retrogradely labelled neurons in the SumL after a dorsal DG injection are FOS+ after PS hypersomnia (Renouard et al. 2015). Finally, it has been shown that all anterogradely labelled fibers localized in the DG after injection of an anterograde tracer in the SumL co-express vGAT, GAD65 and vGLUT2 clearly confirming that the SumL-DG pathway is both GABA and glutamatergic. Altogether, these results

indicate that most SumL neurons projecting to the dDG including those activated during PS hypersomnia have a dual GABA/glutamate phenotype.

In addition, to determine whether SumL neurons are at the origin of all vGLUT2 fibers and induce FOS labelling after PS hypersomnia both in the dDG and vDG, we quantified the number of vGLUT2 fibers and FOS-labelled neurons in these two parts of the DG after full lesions of the Sum. Further, we determined whether the Sum contains retrogradely labelled FOS+ neurons after injection of Fluorogold in the vDG. We found out that Sum lesions induce a nearly complete disappearance and in contrast a non-significance decrease of FOS-labelled neurons in the dorsal and ventral part of the DG, respectively. vGLUT2-labelled fibers also completely disappeared in the dorsal but not in the ventral DG in which they specifically decreased in the supragranular but not in the granular layer itself. Finally, we found only a small number of FOS+ retrogradely labelled neurons in the SumL after injection of Fluorogold in the vDG. Our results are in line with previous studies showing by using anterograde tracer injection that the SumL project more densely to the dorsal than to the ventral DG (Ohara et al. 2013; Soussi et al. 2010; Vertes 1992). They also indicate that all vGLUT2 fibers present in the dorsal but not in the ventral DG originate from Sum neurons. In summary, our results clearly show for the first time that during PS hypersomnia, SumL neurons are fully responsible for the activation of dDG neurons while they play a minor role for that of the vDG neurons.

After injection of Fluorogold in the vDG, a high number of FOS+ retrogradely labelled neurons was specifically observed in the ENTm. Only a few double-labelled neurons were observed in the other afferents to the vDG including the Sum. These results are in line with our previous data showing that the ENTm contains a very large number of FOS+ neurons during PS hypersomnia compared to PS deprivation and control conditions (Renouard et al. 2015). These results contrast with those obtained for the dDG showing that the SumL contains a large number of double-labelled cells while none were observed in the ENTm although it contained a large number of retrogradely labelled neurons (Renouard et al. 2015). Altogether, these results strongly suggest that the ENTm neurons are responsible for the activation of the vDG neurons during PS hypersomnia. These cells might also be at the origin of the remaining vGLUT2 innervation of the vDG after Sum lesion since the ENTm contains vGLUT2+ neurons (Wouterlood et al. 2008).

Functional significance

Our results strongly suggest that bipotential GABA/glutamatergic neurons of the SumL activate the granule cells of the dDG during PS hypersomnia. Further, it is likely that they are also responsible for the previously reported increased expression of BDNF, ARC and COX2 in the granule cells after PS hypersomnia (Renouard et al. 2015). The mechanisms responsible for increased expression of these early genes during PS hypersomnia remain to be determined. Indeed, the expression of FOS and that of the other early genes is generally induced by an increase in firing of the neurons (Yassin et al. 2010). However, activation of the SumL/dDG pathway should induce both the release of GABA and glutamate on dentate granule cells likely resulting in no change in firing rate. Recording of granule cells have shown that they are nearly not active during waking and that they are slightly more active during sleep (Neunuebel and Knierim 2012). Supporting the hypothesis that they do not increase their activity during PS, the downstream targets of DG granule cells, the CA3 neurons do not express FOS during PS hypersomnia (Renouard et al. 2015). In agreement with our results, LFP and unit activity recordings in the hippocampus showed enhanced dentate processing but limited CA3-CA1 coordination and a decrease in CA1 neurons firing rate during PS compared to SWS and WK (Montgomery et al. 2008). We propose that all SumL-dDG terminals corelease GABA and glutamate during PS but that facing GABAergic postsynaptic receptors are located only at somatic level of granule cells whereas NMDA and AMPA glutamatergic receptors are located at dendritic level. In such case, granule cells would be inhibited and therefore not able to generate spikes. However, the activation on DG cells of dendritic NMDA receptors by glutamate during PS hypersomnia could induce calcium entry, activation of the MAP kinase pathway and be responsible for the transcription of immediate early genes including FOS as previously described (Lerea and McNamara 1993). Additional studies on DG neurons across the sleep-waking cycle using calcium imaging, multiunit multisites recordings and optogenetics are needed to test such a hypothesis.

The function of the activation of DG granule cells during PS also remains to be determined. The DG is thought to play a key role in the formation of the contextual component of fear memories by discriminating similar contexts (McHugh et al. 2007). Using early genes expression mapping, it has been shown that the same small group of DG granule cells (2-4%) is activated every time the animal is exposed to the same context while different environments or tasks activate different populations of DG granule cells (Schmidt et al. 2012). Further, it has recently been shown that optogenetic reactivation of DG granule cells activated during fear conditioning is sufficient to induce freezing behaviour (Liu et al. 2012). Conversely,

inactivating DG granule cells that were activated during fear conditioning by optogenetic impairs the expression of the fear memory as evidenced by the lower percentage of freezing when exposing the animals to the same context (Denny et al. 2014). On the other hand, it has been shown that contextual fear conditioning is impaired after PS deprivation (Ravassard et al. 2016) or inhibition of theta rhythm during PS by optogenetic silencing of medial septum GABAergic neurons (Boyce et al. 2016). Altogether, these and our results strongly suggest that activation of DG granule cells during PS plays a role in the consolidation of emotional and spatial memory.

Our results further show that dorsal and ventral DG granule cells are activated during PS by SumL and ENTm neurons, respectively. Interestingly, it has been demonstrated that DG granule cells have different functions along the dorsoventral axis of the hippocampus: dDG neurons seem to control exploratory behavior and encoding of contextual fear memories, while vDG neurons are more implicated in anxiety-related behavior (Kheirbek et al. 2013). Additional studies using optogenetic inhibition and activation of the granule cells of the ventral and dorsal DG activated during PS are necessary to determine whether they play a role in contextual fear memory consolidation and anxiety regulation.

In conclusion, our data strongly suggest that GABA/glutamatergic neurons of the SumL and cortical neurons of the ENTm are responsible for the activation of dorsal and ventral DG granule cells during PS hypersomnia, respectively. Our results open the way to the identification of the functional role of such differential activation of the ventral and dorsal DG granule cells during PS using advanced methods such as optogenetics.

Boyce R, Glasgow SD, Williams S, Adamantidis A (2016) Causal evidence for the role of REM sleep theta rhythm in contextual memory consolidation Science 352:812-816 doi:10.1126/science.aad5252

Denny CA et al. (2014) Hippocampal memory traces are differentially modulated by experience, time, and adult neurogenesis Neuron 83:189-201 doi:10.1016/j.neuron.2014.05.018

Gandrillon O, Solari F, Legrand C, Jurdic P, Samarut J (1996) A rapid and convenient method to prepare DIG-labelled RNA probes for use in non-radioactive in situ hybridization Mol Cell Probes 10:51-55 doi:10.1006/mcpr.1996.0007

Jouvet M, Michel F, Courjon J (1959) Sur un stade d'activité électrique cérébrale rapide au cours du sommeil physiologique CR Seances Soc Biol 153:1024-1028

Kheirbek MA et al. (2013) Differential control of learning and anxiety along the dorsoventral axis of the dentate gyrus Neuron 77:955-968 doi:10.1016/j.neuron.2012.12.038

Kiss J, Csaki A, Bokor H, Shanabrough M, Leranth C (2000) The supramammillo-hippocampal and supramammillo-septal glutamatergic/aspartatergic projections in the rat: a combined [3H]D-aspartate autoradiographic and immunohistochemical study Neuroscience 97:657-669 doi:S0306452200001275 [pii]

Lerea LS, McNamara JO (1993) Ionotropic glutamate receptor subtypes activate c-fos transcription by distinct calcium-requiring intracellular signaling pathways Neuron 10:31-41

Liu X, Ramirez S, Pang PT, Puryear CB, Govindarajan A, Deisseroth K, Tonegawa S (2012) Optogenetic stimulation of a hippocampal engram activates fear memory recall Nature 484:381-385 doi:10.1038/nature11028

McHugh TJ et al. (2007) Dentate gyrus NMDA receptors mediate rapid pattern separation in the hippocampal network Science 317:94-99 doi:10.1126/science.1140263

Montgomery SM, Sirota A, Buzsaki G (2008) Theta and gamma coordination of hippocampal networks during waking and rapid eye movement sleep J Neurosci 28:6731-6741 doi:28/26/6731 [pii]

10.1523/JNEUROSCI.1227-08.2008

Neunuebel JP, Knierim JJ (2012) Spatial firing correlates of physiologically distinct cell types of the rat dentate gyrus J Neurosci 32:3848-3858 doi:10.1523/JNEUROSCI.6038-11.2012

Ohara S, Sato S, Tsutsui K, Witter MP, Iijima T (2013) Organization of multisynaptic inputs to the dorsal and ventral dentate gyrus: retrograde trans-synaptic tracing with rabies virus vector in the rat PLoS One 8:e78928 doi:10.1371/journal.pone.0078928

Ravassard P et al. (2016) REM Sleep-Dependent Bidirectional Regulation of Hippocampal-Based Emotional Memory and LTP Cereb Cortex 26:1488-1500 doi:10.1093/cercor/bhu310

Renouard L et al. (2015) The supramammillary nucleus and the claustrum activate the cortex during REM sleep Science Advances 1 doi:10.1126/sciadv.1400177

Sapin E, Berod A, Leger L, Herman PA, Luppi PH, Peyron C (2010) A Very Large Number of GABAergic Neurons Are Activated in the Tuberal Hypothalamus during Paradoxical (REM) Sleep Hypersomnia PLoS One 5:e11766 doi:10.1371/journal.pone.0011766

Sapin E et al. (2009) Localization of the brainstem GABAergic neurons controlling paradoxical (REM) sleep PLoS ONE 4:e4272 doi:10.1371/journal.pone.0004272

Schmidt B, Marrone DF, Markus EJ (2012) Disambiguating the similar: the dentate gyrus and pattern separation Behav Brain Res 226:56-65 doi:10.1016/j.bbr.2011.08.039

Soussi R, Zhang N, Tahtakran S, Houser CR, Esclapez M (2010) Heterogeneity of the supramammillary-hippocampal pathways: evidence for a unique GABAergic neurotransmitter phenotype and regional differences Eur J Neurosci 32:771-785 doi:EJN7329 [pii]

10.1111/j.1460-9568.2010.07329.x

Swanson LW (1992) Brain maps : structure of the rat brain. Elsevier, New York

Verret L et al. (2003) A role of melanin-concentrating hormone producing neurons in the central regulation of paradoxical sleep BMC Neurosci 4:19

Vertes RP (1992) PHA-L analysis of projections from the supramammillary nucleus in the rat J Comp Neurol 326:595-622

Wouterlood FG et al. (2008) Origin of calretinin-containing, vesicular glutamate transporter 2-coexpressing fiber terminals in the entorhinal cortex of the rat J Comp Neurol 506:359-370 doi:10.1002/cne.21555

Yassin L, Benedetti BL, Jouhanneau JS, Wen JA, Poulet JF, Barth AL (2010) An embedded subnetwork of highly active neurons in the neocortex Neuron 68:1043-1050 doi:S0896-6273(10)00971-2 [pii]

10.1016/j.neuron.2010.11.029

Table 1. Total number of FOS+, FOS/vGLUT2+, vGLUT2+ neurons and percentage of FOS/vGLUT2+ neurons in the supramammillary nucleus of control (PSC), PS deprived (PSD) and hypersomniac (PSR) rats. The neurons were counted on 2 hemi-sections per animal. Values are mean±SEM across 4 animals per group. Significance: Kruskal-Wallis followed by Mann-Whitney. * $p<0.05$ PSR vs PSC, # $p<0.05$ PSR vs PSD. Abbreviations: SumM: medial supramammillary nucleus; SumL: lateral supramammillary nucleus.

Legend for figures:

Fig. 1:

Polygraphic recordings and sleep quantities during the flowerpot paradoxical sleep (PS) deprivation and recovery protocol. **(a, c, e)** Representative electromyogram (EMG) and electroencephalogram (EEG) signals during waking (WK), slow wave sleep (SWS) and PS. **(b, d, f)** Quantities (%) of WK, SWS and PS in control (PSC, n=4), PS deprived rats (PSD, n=4) and rats with PS hypersomnia (PSR, n=12) during the 150 min before euthanasia. Values are mean±SEM. Significance: Kruskal-Wallis followed by Mann-Whitney. ** $p<0.01$ PSR vs PSD, ## $p<0.01$ PSR vs PSC, # $p<0.05$ PSR vs PSC or PSD vs PSC.

Fig. 2:

SumL neurons expressing FOS after PS recovery are glutamatergic and GABAergic. **(a-c)** Schematic distribution of singly FOS+ (black dots), singly vGLUT2+ (green dots) and FOS-vGLUT2 double-labelled (red squares) neurons on a coronal section in a representative animal for PSC (a), PSD (b) and PSR (c) conditions. **(d)** Schematic distribution of singly FOS+ (black dots), singly vGAT+ (green dots) and FOS-vGAT double-labelled (red squares) neurons on a coronal section in a representative PSR animal. **(e)** Photomicrographs showing FOS (brown nuclear staining) and vGLUT2 (blue diffuse cytoplasmic staining) double-stained neurons in the SumL of a PSR rat. **(f)** shows the area inside the rectangle in (e) at a higher magnification. Note the dense cluster of double-labelled neurons in the SumL (red arrowheads). The black and green arrowheads indicate the FOS+ and the vGLUT2+ singly labelled neurons, respectively. **(g)** Photomicrographs showing FOS (brown nuclear staining) and vGAT (blue diffuse cytoplasmic staining) double-stained neurons in the SumL of a PSR rat. **(h)** shows the area inside the rectangle in (f) at a higher magnification. Note the dense cluster of double-labelled neurons in the SumL (red arrowheads). The black arrowheads

indicate the FOS+ singly labelled neurons. Abbreviations: cp: cerebral peduncle; LHA: lateral hypothalamic area; LM: lateral mammillary nucleus; MM: medial mammillary nucleus, medial part; MnM: medial mammillary nucleus, median part; PH: posterior hypothalamic nucleus; pm: principal mammillary tract; SumL: lateral supramammillary nucleus; SumM: medial supramammillary nucleus. Scale bars: 500 µm for (e, g) and 50 µm for (f, h).

Figure 3:

vGLUT2+ fibers and FOS+ neurons are absent in the dorsal DG (dDG) after lesion of the Sum. **(a-d)** Photomicrographs showing vGLUT2 immunostained sections at the level of the dDG in a PSR sham (a, c) and a PSR rat with a lesion of the Sum (b, d). (c) and (d) show the area inside the rectangle in (a) and (b) at a higher magnification. The Sum lesion causes a dramatic reduction in the number of vGLUT2+ fibers in the dDG. **(e-h)** Photomicrographs showing FOS immunostained sections at the level of the dDG in a PSR sham (e, g) and a PSR rat with a lesion of the Sum (f, h). (g) and (h) show the area inside the rectangle in (e) and (f) at a higher magnification. The Sum lesion causes a dramatic reduction in the number of FOS+ neurons in the dDG. **(i)** Illustration of a representative neurotoxic lesion of the Sum on a section immunostained with NeuN. **(j)** Mean±SEM optic density of vGLUT2 staining and number of FOS+ neurons in dDG in rats with a Sum lesion (n=4) relative to PSR sham animals (n=4). Significance: Kruskal-Wallis followed by Mann-Whitney. * $p<0.05$. Abbreviations: CA3: field CA3, Ammon's Horn; DGlb: dentate gyrus, lateral blade; DGlb-mo: dentate gyrus, lateral blade-molecular layer; DGlb-sg: dentate gyrus, lateral blade-granule cell layer; DGmb: dentate gyrus, medial blade; DGmb-mo dentate gyrus, medial blade-molecular layer; DGmb-po: dentate gyrus, medial blade-polymorph layer; DGmb-sg: dentate gyrus, medial blade-granule cell layer; LM: lateral mammillary nucleus; MM: medial mammillary nucleus, medial part; MnM: medial mammillary nucleus, median part; pm: principal mammillary tract; SumL: lateral supramammillary nucleus; SumM: medial supramammillary nucleus; V3: third ventricle. Scale bars: 500 µm for (a, b, e, f, i); 50 µm for (c, d, g, h).

Figure 4:

vGLUT2+ fibers and FOS+ neurons are present in the ventral DG (vDG) after lesion of the Sum. **(a-d)** Photomicrographs showing the vGLUT2 staining in a representative PSR sham (a, c) and a PSR rat with a Sum lesion (b, d). The Sum lesion does not induce a significant

reduction in the number of vGLUT2+ fibers in the vDG. (c) and (d) show the area inside the rectangle in (a) and (b) at a higher magnification. **(e-h)** Photomicrographs showing FOS immunostained sections at the level of the vDG in a PSR sham (e, g) and a PSR rat with a lesion of the Sum (f, h). (g) and (h) show the area inside the rectangle in (e) and (f) at a higher magnification. The Sum lesion does not cause a reduction in the number of FOS+ neurons in the vDG. **(i)** Schematic distribution of FOS+ (black dots) neurons in the dDG and vDG on a coronal section in a sham (left) and a lesioned (right) rat. Note the strong decrease in the number of FOS+ neurons in the dDG but not the vDG. **(j)** Mean±SEM optic density of vGLUT2 staining and number of FOS neurons in vDG in rats with a Sum lesion (n=4) relative to PSR sham animals (n=4). Abbreviations: CA3: field CA3, Ammon's Horn; dDG: dorsal dentate gyrus; DGlb: dentate gyrus, lateral blade; DGlb-mo: dentate gyrus, lateral blade-molecular layer; DGlb-sg: dentate gyrus, lateral blade-granule cell layer; DGmb: dentate gyrus, medial blade; DGmb-mo: dentate gyrus, medial blade-molecular layer; DGmb-po: dentate gyrus, medial blade-polymorph layer; DGmb-sg: dentate gyrus, medial blade-granule cell layer; vDG: ventral dentate gyrus. Scale bars: 500 µm for (a, b, e, f); 50 µm for (c, d, g, h).

Figure 5:

The FOS+ neurons projecting to the vDG in PSR animals are mostly located in the medial entorhinal cortex. **(a, c, e)** Schematic distribution of singly FOS+ (black dots), singly FG+ (green dots) and FOS-FG double-labelled (red squares) neurons in the medial septum (a), the Sum (c) and the entorhinal cortex (e) in a representative PSR animal. **(b, d, f)** Photomicrographs showing FOS (black nuclear staining) and FG (brown cytoplasmatic staining) double-stained neurons in the medial septum (b), the Sum (d) and the entorhinal cortex (f) of a PSR rat. Note the dense cluster of double-labelled neurons in the medial entorhinal cortex (red arrowheads)**.** The black and green arrowheads indicate the FOS+ and FG+ singly labelled neurons, respectively. **(g)** Photomicrograph showing a representative FG injection in the vDG. **(h)** Mean±SEM number of FOS/FG+ cells contained in the structures projecting to the vDG. Abbreviations: BST: bed nuclei stria terminalis; cp: cerebral peduncle; DGlb: dentate gyrus, lateral blade; DGlb-mo: dentate gyrus, lateral blade-molecular layer; DGlb-sg: dentate gyrus, lateral blade-granule cell layer; DGmb: dentate gyrus, medial blade; DGmb-mo: dentate gyrus, medial blade-molecular layer; DGmb-po: dentate gyrus, medial blade-polymorph layer; DGmb-sg: dentate gyrus, medial blade-granule cell layer; ECT: ectorhinal area; ENTl: entorhinal area, lateral part; ENTm: entorhinal area, medial part; IPN:

interpeduncular nucleus; LHA: lateral hypothalamic area; LM: lateral mammillary nucleus; LS: lateral septal nucleus; MS: medial septal nucleus; MM: medial mammillary nucleus, medial part; MnM: medial mammillary nucleus, median part; NBD: diagonal band nucleus; PAR: parasubiculum; PH: posterior hypothalamic nucleus; pm: principal mammillary tract; SF: septofimbrial nucleus; SUBv: subiculum, ventral part; SumL: lateral supramammillary nucleus; SumM: medial supramammillary nucleus; VL: lateral ventricle. Scale bars: 500 μm for (b, d, f, g); 50 μm for the insets.

	PSC	PSD	PSR
SumM			
FOS +	14,2 ± 8,1	40,2 ± 10,4	22,5 ± 1,8
FOS/vGLUT2 +	5,2 ± 3,3	15,2 ± 4,6	12 ± 4,4
vGLUT2 +	8,2 ± 2,4	8,7 ± 3,7	2,2 ± 1,3
% FOS/vGLUT2 +	36,8 ± 12,3	37,9 ± 9,5	53,3 ± 17,5
SumL			
FOS +	37 ± 16,5	56 ± 19,4	112,2 ± 11,7 * #
FOS/vGLUT2 +	22 ± 7,9	29,5 ± 11,5	94,5 ± 11,9 * #
vGLUT2 +	59,5 ± 12,3	58,7 ± 12,1	33 ± 10,1
% FOS/vGLUT2 +	59,5 ± 10,7	52,7 ± 11,2	84,2 ± 4,3

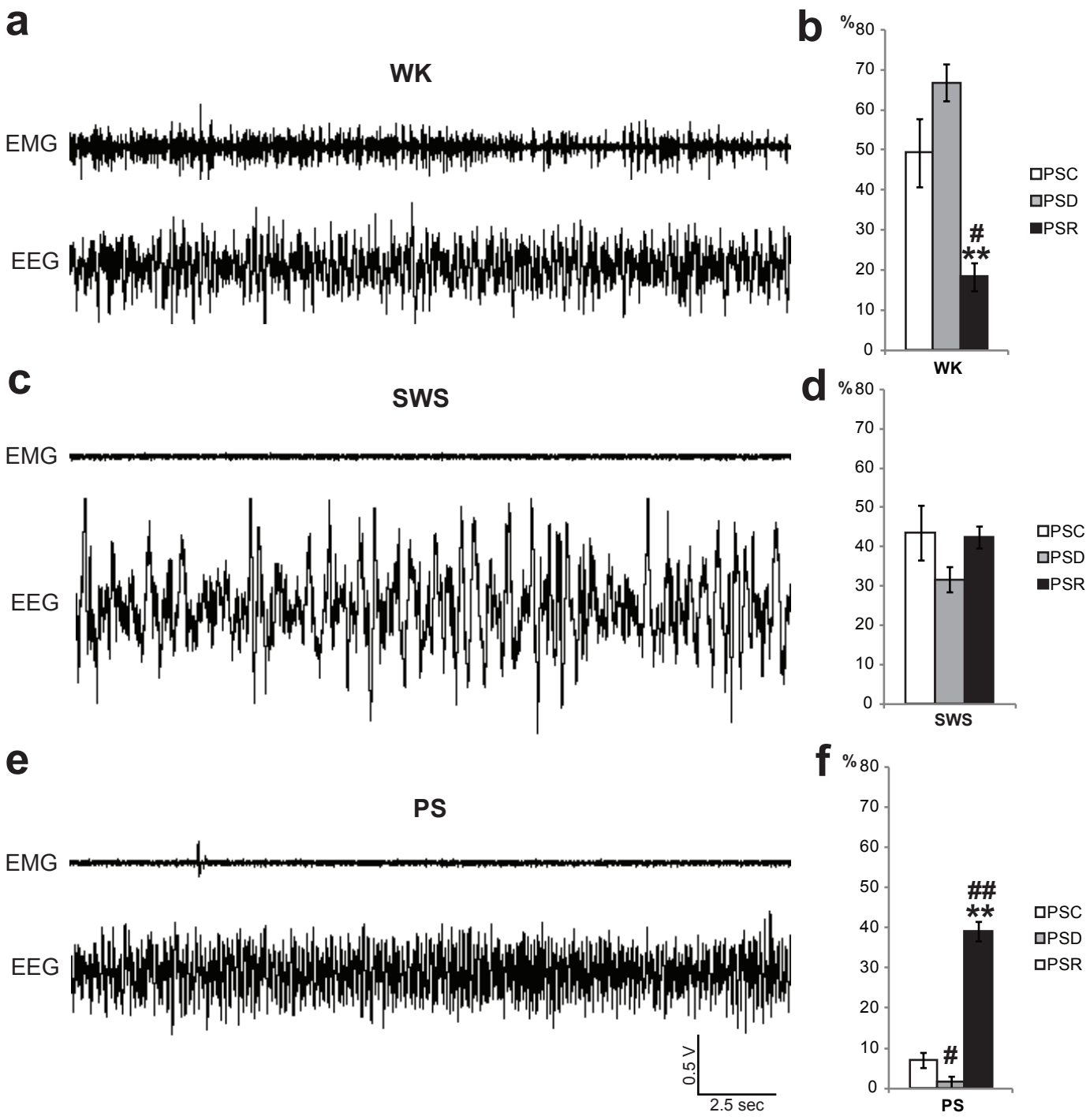
a
WK
EMG
EEG
b
%
80
70
60
50
40
30
20
10
0
#
**
PSC
PSD
PSR
WK
c
SWS
EMG
EEG
d
%
80
70
60
50
40
30
20
10
0
PSC
PSD
PSR
SWS
e
PS
EMG
EEG
0.5 V
2.5 sec
f
%
80
70
60
50
40
30
20
10
0
##
**
#
PSC
PSD
PSR
PS

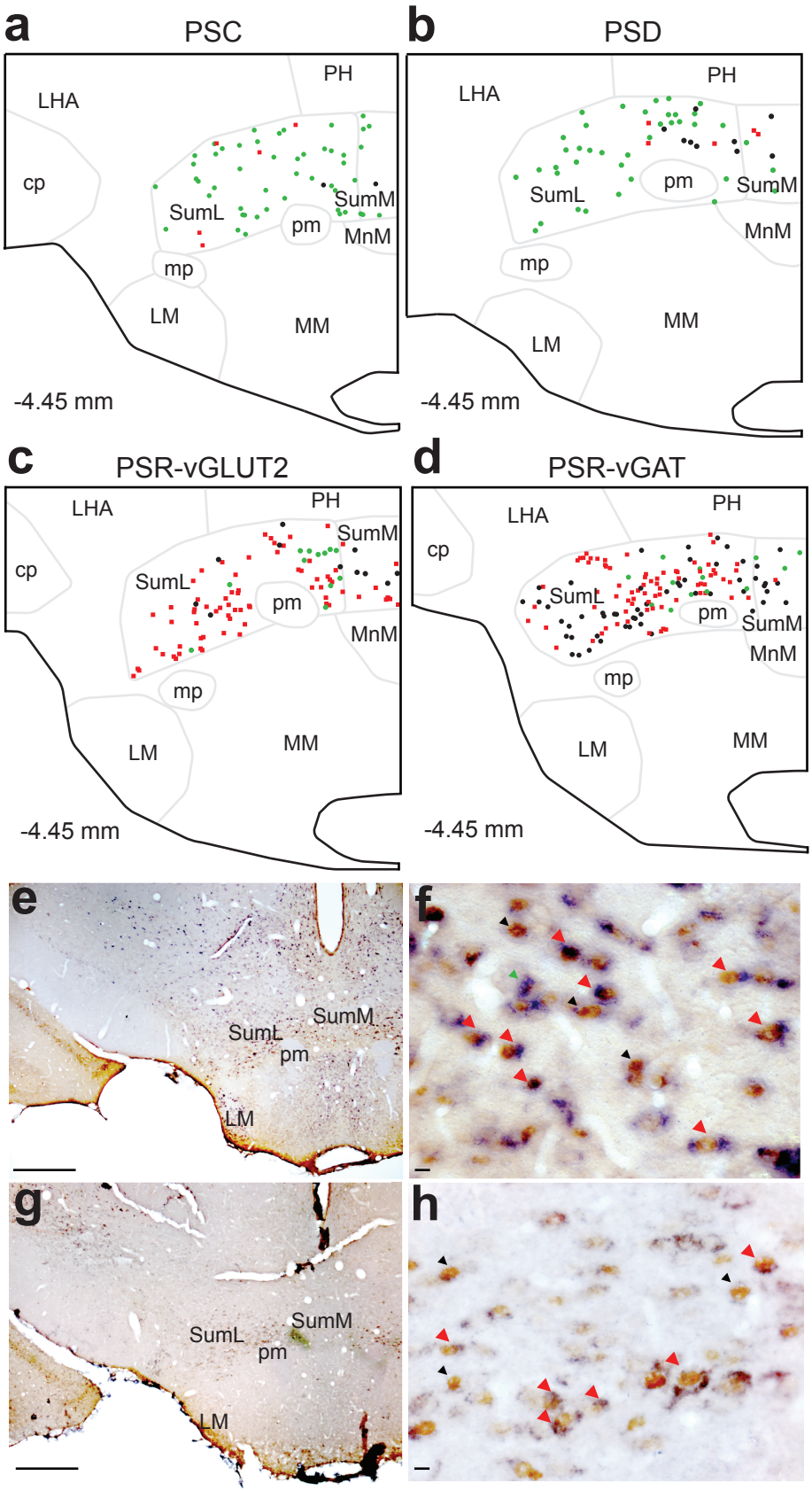
a
PSC
PH
LHA
cp
SumL
SumM
pm
MnM
mp
LM
MM
-4.45 mm
b
PSD
PH
LHA
SumL
pm
SumM
MnM
mp
LM
MM
-4.45 mm
c
PSR-vGLUT2
LHA
PH
SumM
cp
SumL
pm
MnM
mp
LM
MM
-4.45 mm
d
PSR-vGAT
LHA
PH
cp
SumL
pm
SumM
MnM
mp
LM
MM
-4.45 mm
e
SumM
SumL
pm
LM
f
g
SumL
SumM
pm
LM
h

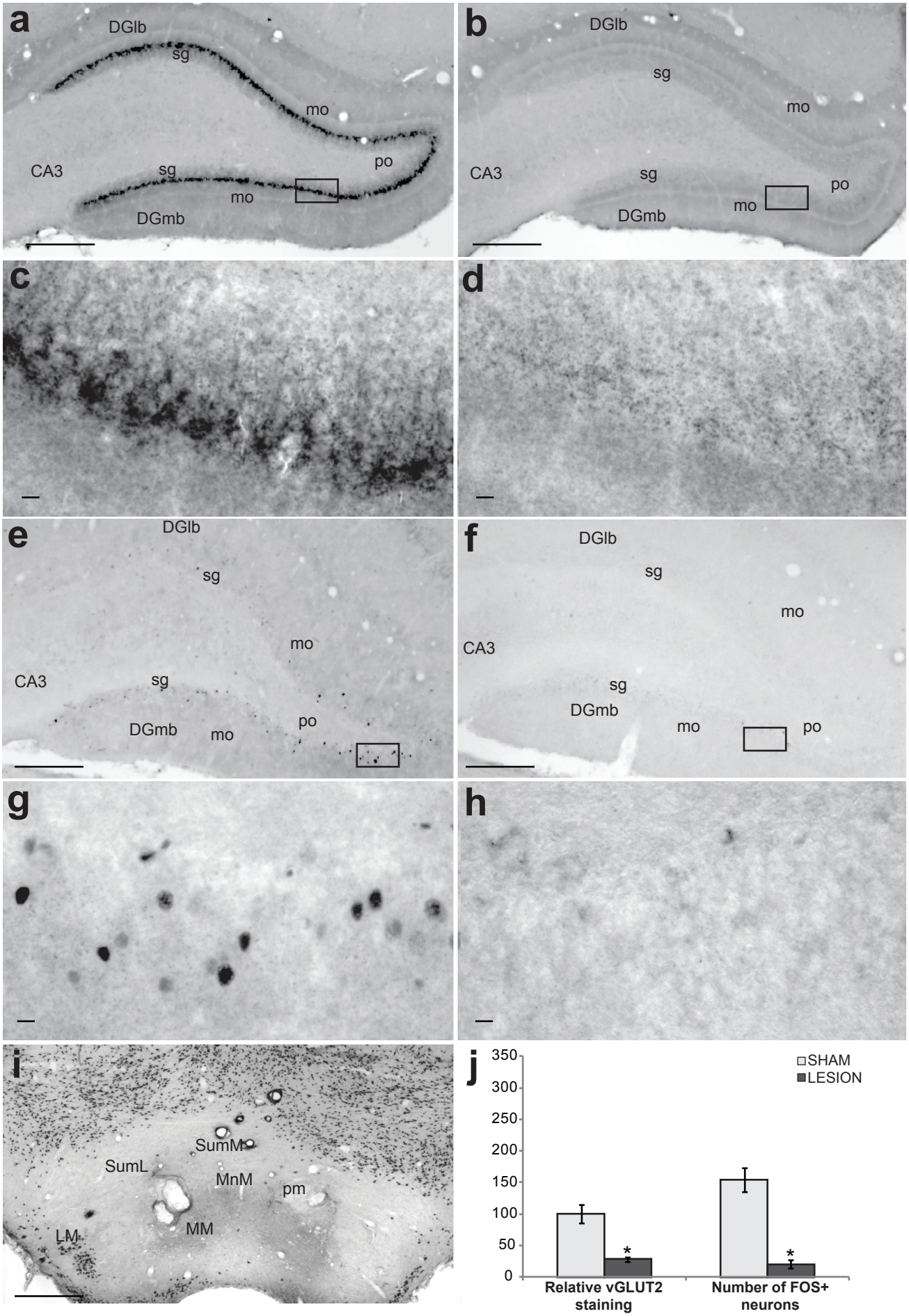
a
DGlb
sg
mo
po
CA3
sg
mo
DGmb
b
DGlb
sg
mo
CA3
sg
po
mo
DGmb
c
d
e
DGlb
sg
mo
CA3
sg
DGmb
mo
po
f
DGlb
sg
mo
CA3
sg
DGmb
mo
po
g
h
i
SumM
SumL
MnM
pm
MM
LM
j
350
300
250
200
150
100
50
0
SHAM
LESION
*
*
Relative vGLUT2 staining
Number of FOS+ neurons

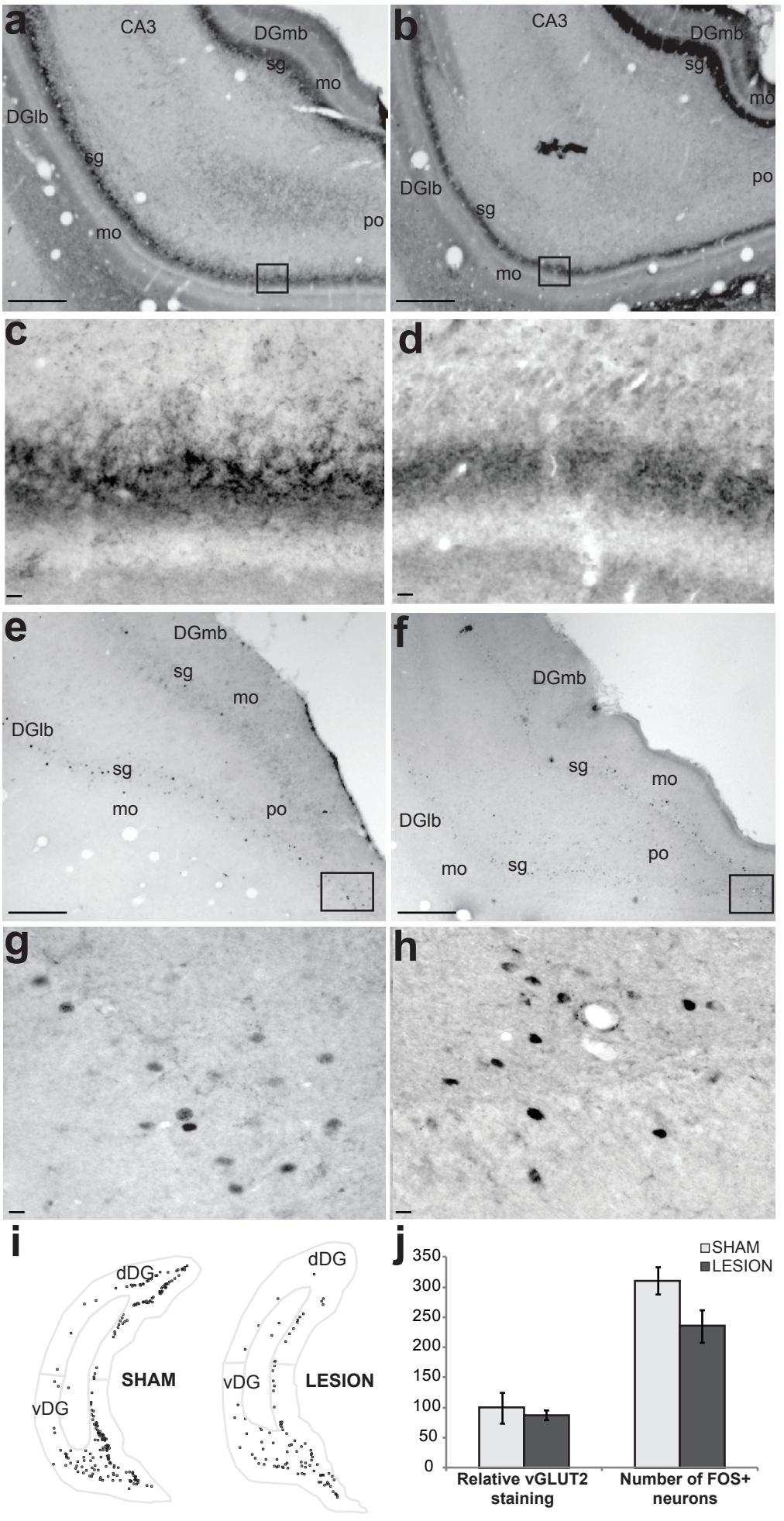
a
CA3
DGmb
sg
mo
DGlb
sg
mo
po
b
CA3
DGmb
sg
mo
po
DGlb
sg
mo
c
d
e
DGmb
sg
mo
DGlb
sg
mo
po
f
DGmb
sg
mo
DGlb
po
mo
sg
g
h
i
dDG
SHAM
vDG
dDG
vDG
LESION
j
350
300
250
200
150
100
50
0
SHAM
LESION
Relative vGLUT2 staining
Number of FOS+ neurons

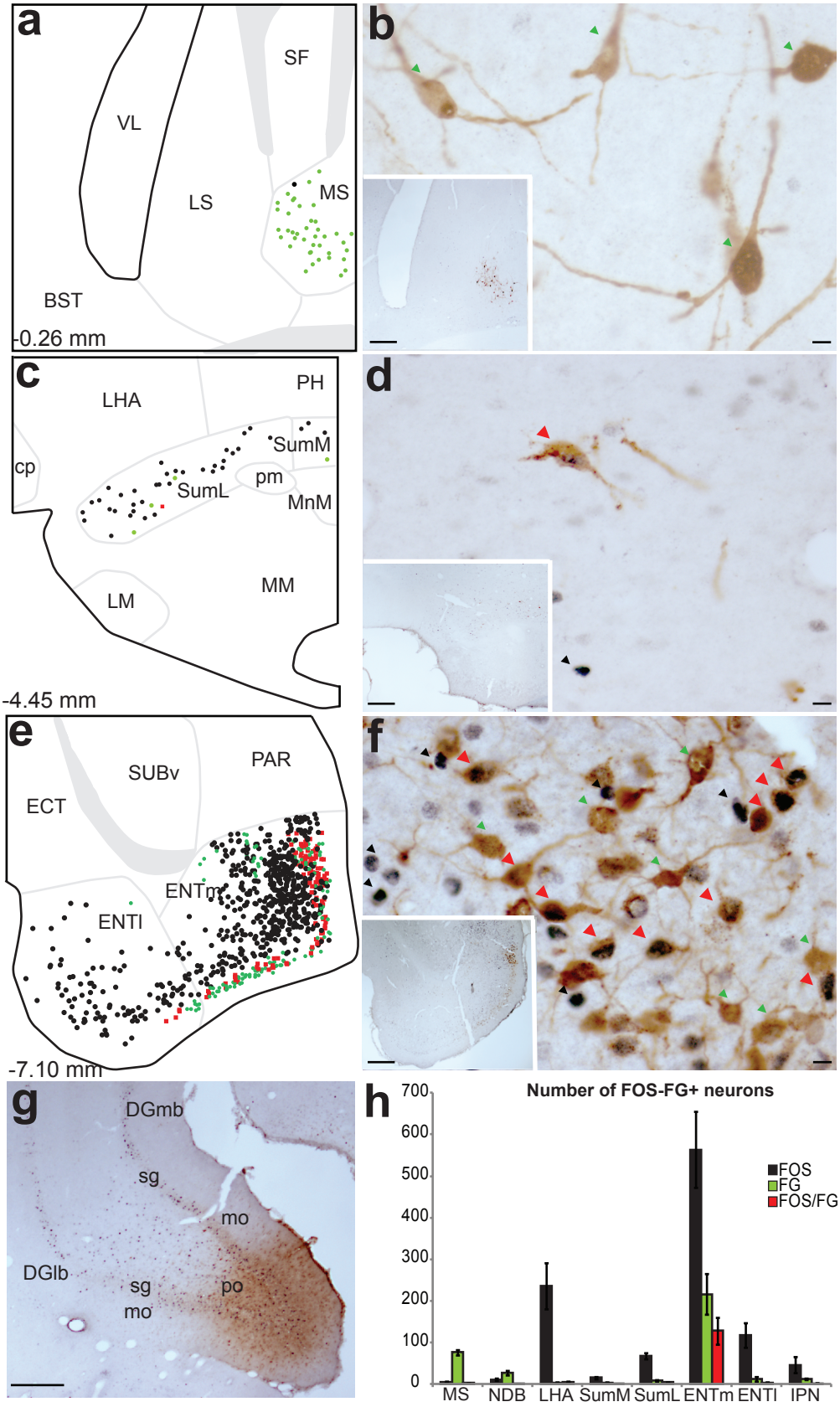
a
SF
VL
LS
MS
BST
-0.26 mm
b
c
LHA
PH
SumM
cp
pm
SumL
MnM
MM
LM
-4.45 mm
d
e
SUBv
PAR
ECT
ENTm
ENTl
-7.10 mm
f
g
DGmb
sg
mo
DGlb
sg
po
mo
h
Number of FOS-FG+ neurons
700
600
500
400
300
200
100
0
FOS
FG
FOS/FG
MS
NDB
LHA
SumM
SumL
ENTm
ENTl
IPN